Detecting cold dark-matter candidates

Andrzej K. Drukier

Max-Planck-Institut für Physik und Astrophysik, 8046 Garching, West Germany
and Department of Astronomy, Harvard-Smithsonian Center for Astrophysics,
60 Garden Street, Cambridge, Massachusetts 02138

Katherine Freese and David N. Spergel

Department of Astronomy, Harvard-Smithsonian Center for Astrophysics, 60 Garden Street,
Cambridge, Massachusetts 02138

We consider the use of superheated superconducting colloids as detectors of weakly interacting galactic-halo candidate particles (e.g., photinos, massive neutrinos, and scalar neutrinos). We discuss realistic models for the detector and for the galactic halo. We show that the expected count rate ($\approx 10^3$ count/day for scalar and massive neutrinos) exceeds the expected background by several orders of magnitude. For photinos, we expect ≈ 1 count/day, more than 100 times the predicted background rate. We find that if the detector temperature is maintained at 50 mK and using SQUID electronic read out with the system, noise is reduced below 5×10^{-4} flux quanta, particles with mass as low as 2 GeV can be detected. Any particle capable of resolving the solar-neutrino problem by altering energy transport in the Sun can be detected. We show that Earth's motion around the Sun can produce a significant annual modulation in the signal.

I. INTRODUCTION

Drukier and Stodolsky[1] proposed low-temperature particle detectors, specifically superheated superconducting colloid detectors (SSCD's), for the detection of MeV-range neutrinos through elastic scattering on nuclei and identification of the recoil energy. The SSCD consists of superconducting grains maintained just below the transition temperature; the energy deposited in a grain by the elastic scattering of a weakly interacting particle raises the temperature in the grain sufficiently to cause it to go normal. The penetration of magnetic flux into the grain then produces an observable signal on the read-out electronics (SQUID's, superconducting quantum interference devices). Goodman and Witten[2] showed that the SSCD can be used to detect several candidates for the dark matter in the galactic hallo: particles in the GeV mass range with coherent weak interactions (e.g., massive neutrinos and scalar neutrinos), spin-dependent interactions of typical weak strength (e.g., photinos), or strongly interacting particles. Similar calculations have been carried out by Wasserman.[2] In this paper we examine the capability of the SSCD for detection of these candidate particles with realistic models for the detector and for the velocity distribution in the galactic halo.

In Sec. II we discuss the various components of the detection system and their effects on detection capabilities. In particular, we find a strong dependence of detector response on the velocity of the incoming particle, count rate $\propto v^7$. Hence we are driven to a discussion in Sec. III of a realistic model of the local distribution of velocities for the galactic halo. In Sec. IV we evaluate cross sections for elastic scattering on nuclei for several candidate particles: massive neutrinos and various possible lightest supersymmetric particles, scalar neutrinos, photinos, and Higgs fermions.

In Sec. V we estimate the contributions to the signal from various backgrounds. Because the signature for an event is the flip of just one grain, the background from most cosmic rays and radioactive decays can be recognized as the flipping of multiple grains and can be immediately rejected. A possible source of background, solar neutrinos, is shown to be negligible. The motion of the Earth around the Sun produces a modulation in the dark-matter count rate. We discuss using this modulation to enhance background subtraction and confirm a detection.

Using the results of the previous sections, we then calculate in Sec. VI expected count rates in the detector. If the dominant component of the halo consists of either massive or scalar neutrinos of mass > 5 GeV, a 1-kg detector would record 10^4 counts per day; if the halo consists predominantly of photinos, we expect a few counts/kg day. By reducing the SQUID noise and the system temperature, the minimum detectable mass can be pushed down to 2 GeV. Section VII sums up the paper.

II. THE DETECTOR

The identification of an elastic neutral-current scattering of a GeV-mass particle with a heavy nucleus requires a detector with sensitivity to heavy nuclei recoils with energies < 1 keV, and good background rejection. Unfortunately, conventional particle detectors with the possible exception of low-gap semiconductors do not satisfy these conditions. However, low-temperature particle detectors, specifically, superheated superconducting colloid detectors[1] (SSCD's), satisfy these requirements for an effective detector of weakly interacting particles of several GeV.

In Secs. VI and VII we also discuss the crystal bolometers and show that the most popular ones, Si and Ge, have cross sections considerably smaller than the best superconducting detectors. Furthermore, the challenges of radioactive background suppression in diverse low-temperature detectors are discussed.

The SSCD consists of superconducting grains, a few μm in diameter, embedded in a dielectric material, and placed in a magnetic field. The grains are maintained just below their superconducting transition temperature. The incident halo particle scatters off of a nucleus in the grain, imparting a recoil energy of a few hundred eV. This small energy deposition is sufficient to make a tiny superconducting grain go normal, permitting the magnetic flux to penetrate into the grain and producing an electromagnetic signal in the read-out electronics.

The detector is characterized by an energy threshold E_{th}:

$$E_{\text{th}} \approx \frac{4\pi}{3} r_g{}^3 C_V(T)\Delta T , \tag{1}$$

where r_g is the radius of the grain, $C_V(T)$ is the specific heat of the metal, and ΔT is a function of the external magnetic field. Any collision that imparts a recoil energy above the energy threshold produces a detectable signal. Because of variations that occur in grain preparation, there will be a spread of approximately 20% in the grain energy thresholds within a detector.

The recoil energy transferred in a collision between an incident particle of mass m and velocity v and a grain composed of nuclei of mass M depends upon the scattering angle θ:

$$E_{\text{recoil}} = \frac{m^2 M}{(m+M)^2} v^2(1-\cos\theta) . \tag{2}$$

Thus, the maximum recoil energy is

$$E_{\text{max}} = \frac{2m^2 M}{(m+M)^2} v^2 . \tag{3a}$$

Since a particle can be detected only if it deposits more than E_{th} in a scattering, there is a minimum detectable velocity v_{min}:

$$v_{\text{min}}{}^2 = \frac{(m+M)^2 E_{\text{th}}}{2m^2 M} . \tag{3b}$$

Therefore, a particle is detectable only if its mass is large enough so that there are incident particles with velocities greater than v_{min}:

$$m \geq \frac{M}{(2Mv_{\text{max}}{}^2/E_{\text{th}})^{1/2} - 1} , \tag{4}$$

v_{max} is the maximum particle velocity which for halo particles is the local escape velocity from the galaxy. We see that particle detectability depends upon (1) particle mass and velocity, (2) choice of grain material, (3) system temperature and imposed magnetic field, and (4) the size of the grains. We will see that the minimal size of the grains is set by the sensitivity of the read-out electronics.

There are over 20 elements that are type-I superconductors. The grains in the detectors can be composed of any

one of these elements. Since these elements vary by 1—2 orders of magnitude in specific heat, atomic number, density, critical temperature, and critical magnetic fields, different materials are optimal for different detector tasks. Furthermore, the level of contamination of naturally occurring radioactive elements, potassium, uranium, and thorium, vary from metal to metal, thus the expected level of background counts varies from element to element. Tin, because of its very low specific heat ($C_V = 34$ eV/μm^3 K at 50 mK) and its relatively high critical field ($H_c = 303$ G), makes an excellent detector of both scalar and massive neutrinos.[1] Other advantages of tin are its low melting point which facilitates grain production and extensive experience in using tin SCCS's. The high aluminum-photino scattering cross section makes it an excellent candidate for use in the detection of photinos.

The energy threshold depends strongly on the system temperature, $E_{\text{th}} \propto C_V(T)\Delta T \propto T^2$ for $T \leq 1$ K. Particles with mass greater than 20 GeV can be detected[1] by a detector cooled to 0.4 K. Detection of particles of masses less than 5 GeV necessitates working in lower temperatures. Throughout this paper, we will assume $T = 50$ mK, a system temperature easily obtained in commercially available dilution refrigerators for mass samples smaller than 10 kg. These cryostats have a temperature stability of better than 1 mK. There are several sources of thermal noise: the temperature instability of the helium bath, temperature fluctuations, and external phonon absorption. If we require that the grain must be heated by at least 12.5 mK to produce a change of state, these temperature noise effects are negligible.[1]

The disappearance of the Meissner effect signals the change of state of a grain due to an elastic collision. The superconducting grain placed in the external magnetic field H is equivalent to a magnetic dipole; the disappearance of this dipole generates a detectable emf. Since the grains are in a metastable superheated state, the change of magnetic permeability is permanent, and thus can be conveniently detected by SQUID's. We can determine the change in flux at the loop induced by the change in state of a single grain of radius r_g (and volume V_g) inside a circular loop of radius r_L:

$$\Delta\phi_{\text{loop}} = -\frac{HV_g}{2r_L}\left[\frac{E(k)}{1-a} + \frac{K(k)}{1+a}\right] , \tag{5}$$

where a, d, and k are defined in terms of A, the distance from the grain to the loop axis and D, the distance from the grain to loop plane: $a = A/r_L$, $d = D/r_L$, and $k^2 = 4a/[(1+a)^2 + d^2]$. $E(k)$ and $K(k)$ are elliptical integrals. For a grain in the center of the loop, this simplifies to

$$\Delta\phi_{\text{loop}} = -\Delta\phi_g \frac{r_g}{r_L} , \tag{6}$$

where $\Delta\phi_g \approx \pi r_g{}^2 H$.

If the "flux sensitivity" of the SQUID is assumed to be constant, then the optimum sensitivity will be obtained when $\Delta\phi_{\text{SQUID}}$ is maximized. This can be done by either varying the number of turns in the pickup coil or by varying L_{SQUID} which requires rebuilding the SQUID, but is

sometimes possible and useful. The change in flux observed by the SQUID will depend upon the number of turns in the loop, the inductances of the SQUID (L_{SQUID}), and the inductance of a single turn in the loop L_1:

$$\Delta\phi_{\mathrm{SQUID}} = -\frac{k}{2}\left[\frac{L_{\mathrm{SQUID}}}{L_1}\right]^{1/2}\Delta\phi_{\mathrm{loop}}$$

$$= F_{\mathrm{SQUID}}\Delta\phi_{\mathrm{loop}} , \qquad (7)$$

where $|k| \leq 1$. F_{SQUID}, the figure of merit of the SQUID read-out system, will be assumed to be 0.3 for loops of radius 10 cm and 0.215 for loops of radius 20 cm.

We will require that the signal produced in the SQUID by a grain flip $\Delta\phi_{\mathrm{SQUID}}$ exceed the system noise by a factor 10. The intrinsic noise in a dc SQUID is very small:

$$\Delta\phi_{\mathrm{noise}} \approx 5 \times 10^{-6}\phi_0/\sqrt{\mathrm{Hz}} , \qquad (8)$$

where $\phi_0 = 2.07 \times 10^{-7}$ G cm^2 is a flux quantum. For loops with a radius greater than 10 cm, other sources of noise, mechanical vibrations, and the pickup of magnetospheric fluctuations, dominate and contribute between 10^{-4} and 10^{-2} flux quanta per $\sqrt{\mathrm{Hz}}$. Thus the choice of loop diameter and the observed read-out system noise defines the minimal size of the grain and the energy threshold. In Fig. 1, E_{th} is plotted as a function of read-out system noise for a tin detector with loops of radius 10 and 20 cm. Figure 2 is the same plot for an aluminum detector.

The optimal read-out configuration may consist of several small read-out loops in parallel. Magnetic gradiometers can be used to reject external magnetic noise. These improvements would reduce the $\Delta\phi_{\mathrm{loop}}$ required for a clean detection, and, hence, allow the use of smaller grains and the detection of less massive particles.

Natural radioactivity is the major source of background. Radioactive decays produce particles with kinetic energies of many MeV. These particles are likely to flip
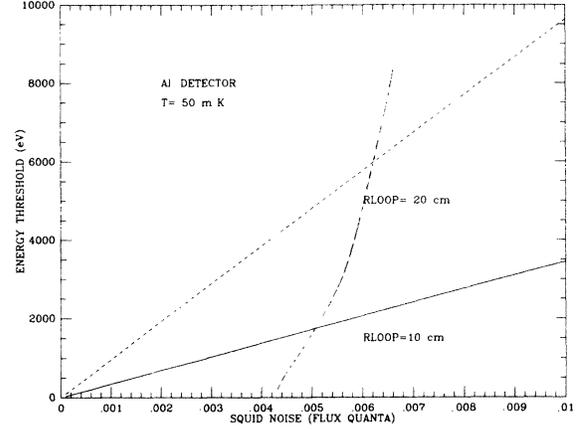
FIG. 2. Same as Fig. 1 for an aluminum detector.

not one but many grains. For example, the requirement that only one grain flips diminishes the background due to ^{40}K impurities by 4 orders of magnitude. By filling only a fraction of the volume of the loop with the colloid, and by requiring that both the multiple flippings of grains and the flipping of a single grain near the surface of the colloid (which produces a stronger signal) are rejected, the contribution of natural radioactivity to the background can be markedly reduced.[1] Numerical analysis shows that the optimal detector looks like the surface of revolution of a filled pretzel and occupies 30% of the loop volume.

Only a small fraction of the colloid ($\approx 10\%$) is composed of superconducting grains, the rest of the colloid is composed of the dielectric, which prevents grains from transferring heat to their neighbors. Thus only a small fraction of the volume of the loop is allotted to grains. The count rate per SQUID will scale with the mass of the grains within the loop connected to the SQUID. The mass of superconducting grains within each loop M_d depends upon the filling factor of grains in the colloid α_{coll} and the fraction of the volume of the detector allocated to the colloid α_{loop}:

$$M_d = \frac{4\pi}{3}r_L^3\rho\alpha_{\mathrm{coll}}\alpha_{\mathrm{loop}} \approx 0.04\pi\rho r_L^3 , \qquad (9)$$

where ρ is the density of the element used in the superconducting grain.

Because of the high cost of the SQUID's and the difficulties of operating more than ten SQUID read-out systems, we wish to maximize the count rate per SQUID. Since the count rate scales as the mass of the detector and the incident particle velocity, we wish to maximize M_d. Equation (9) shows that $M_d \propto r_L^3$. If a larger loop is used, maintaining the same signal strength $\Delta\phi_{\mathrm{SQUID}}$ requires larger grains. Equations (6) and (7) yield $r_L \propto r_g^3$ if all the other parameters of the detector are held constant. Since it takes more energy to heat a larger grain, the price of a large loop is a higher-energy threshold. Since $E_{\mathrm{th}} \propto m_{\mathrm{grain}} \propto r_g^3$, $M_d \propto E_{\mathrm{th}}^3$. For a dark-matter particle of given mass, the energy threshold establishes a minimum detectable particle velocity v_{min}; Eq. 3(b) yields $E_{\mathrm{th}} \propto v_{\mathrm{min}}^2$. Hence, from Eqs. (1)—(9) we see that the
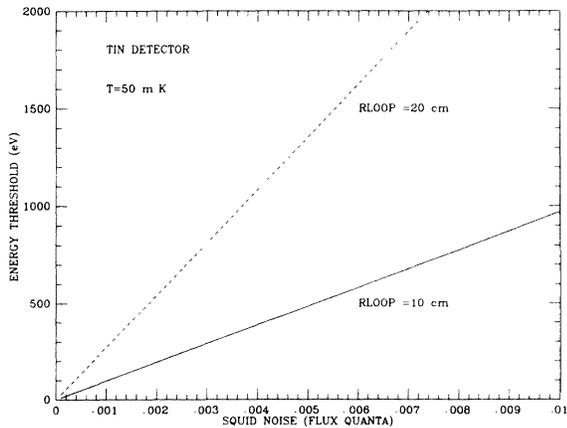

FIG. 1. Energy threshold (in eV) as a function of read-out system noise for a tin detector with loops of radius 10 and 20 cm. Noise is taken to vary between $(10^{-2}-10^{-4})\phi_0$ where a flux quantum $\phi_0 = 2.07 \times 10^{-7}$ G cm.

mass of grains attached to each SQUID scales as $v_{\min}{}^6$:

$$M_d = \frac{9\pi}{250}\rho\alpha_{\text{coll}}\alpha_{\text{loop}}$$

$$\times \left[\frac{F_{\text{SQUID}}H}{\Delta\phi_{\text{noise}}}\frac{m^2M}{(m+M)^2}\frac{1}{C_V(T)\Delta T}\right]^3 v_{\min}{}^6 . \quad (10)$$

This strong velocity dependence encourages the use of a realistic model of the local distribution of velocities for the galactic halo, the subject of the next section.

III. THE HALO MODEL

In discussing particle detectability, Goodman and Witten[2] assumed that the halo is composed of particles with velocities ≈ 200 km sec^{-1}. Because of the strong sensitivity of the system to particle velocity, we are motivated to use a more realistic model of the local distribution of dark matter.

Our Galaxy is a spiral galaxy. Most of its luminosity is produced in metal-rich stars distributed in a disk. Our Sun is part of this disk, which consists mostly of stars and gas clouds orbiting the galactic center in nearly circular orbits. The luminosity of spiral disks is observed to fall off exponentially with radius. While most of the luminosity is produced in a thin disk, most of the mass in the Galaxy is in a nonluminous, perhaps nonbaryonic halo.[3] Observations[4] of the rotation curves of other spiral galaxies (circular velocity v_c as a function of radius) determine the distribution of mass in a galaxy as a function of radius R through straightforward orbital dynamics:

$$\frac{GM(R)}{R^2} = \frac{v_c(R)^2}{R} . \quad (11)$$

In a wide range of spiral galaxies, the rotation curve is flat: the circular speed is independent of radius.[5] This implies that $M(R) \propto R$; thus galaxies are observed to have a halo of nonluminous matter, whose density falls off as R^{-2} out to the edge of the Galaxy. If photinos or scalar neutrinos make a significant contribution to the density of the Universe, we expect them to be the major component of the halo.

Oort[6] was the first to infer the local density distribution through a detailed study of stellar motions. Oort noted that stars in the Galaxy should be in hydrostatic equilibrium. Any stellar population in equilibrium in our galactic disk will satisfy

$$\frac{d[n(z)\langle v_z^2(z)\rangle]}{dz} = n(z)\frac{d\phi}{dz} , \quad (12)$$

where $n(z)$ is the stellar density as a function of height above the disc z, v_z is the stellar velocity perpendicular to the disk, and ϕ is the galactic potential. Through Poisson's equation, Oort inferred the local density distribution. This technique[6] has been refined by using better samples and treating the problem self-consistently.

Several authors[7,8] have made detailed models of the distribution of mass in our Galaxy. Caldwell and Ostriker[7] estimate a local halo density: ρ_{halo} of $0.007 M_\odot/\text{pc}^3 = 0.4$ GeV/cm^3. There is a factor 2 uncertainty in this esti-

mate. This is the largest uncertainty in our halo model.

Unlike the disk of the Galaxy, which is supported against radial collapse by its angular momentum, the dark halo is supported by random velocity which serves as a collisionless pressure. We will assume that the halo is isotropic and spherically symmetric (see also Appendix). We can again apply the equation of hydrostatic balance (this time in the radial direction):

$$\frac{d[n(R)\langle v_R^2\rangle]}{dR} = n(R)\frac{d\phi}{dR} . \quad (13)$$

Applying Eq. (11), and recalling that the halo density is observed to fall off as R^{-2} in other galaxies, we can determine the radial velocity dispersion:

$$\langle v_R^2\rangle = -\frac{d[\ln(R)]}{d[\ln(n)]}v_c^2 = \tfrac{1}{2}v_c^2 . \quad (14)$$

We have assumed that the radial velocity dispersion is independent of radius. The local circular speed is observed to be 243 ± 20 km/sec (Ref. 9).

When the matter that makes up the halo collapsed to form our Galaxy, the velocities of its constituent particles (photinos, axions, black holes?) were randomized in a process called "violent relaxation."[10] Since the particles of interest to our detector, photinos, scalar neutrinos, and massive neutrinos, have such small cross sections that their time scale for collisions with interstellar baryons exceeds the age of the Universe by many orders of magnitudes, they retain the velocity distribution function obtained during the formation of our Galaxy.

While we do not know the details of the halo-distribution function, we are able to infer its general structure. It must be a decreasing function of energy.[11] If we assume that collapse has nearly isotropized the distribution function, we can infer that the total velocity dispersion is approximately three times the radial velocity dispersion, thus ≈ 300 km sec^{-1}. We know that particles whose velocities exceed the galactic escape velocity will have escaped; therefore, the distribution function must be truncated at the escape velocity.

If we assume that the halo-distribution function depends only on cosmion energy, then we can invert the density profile to find the velocity distribution. An r^{-2} halo is produced by the standard isothermal sphere model for the halo velocity distribution. Such a model self-consistently generates a flat rotation curve.

Unlike the disk, the halo is not rotating. If the halo did rotate, it would be flattened like the disk. This is inconsistent with several observations: The scale height of the HI gas in our own Galaxy is observed to increase rapidly outside a radius of 10 kpc where the spheroidal halo begins to dominate the potential in the galactic plane. Observations of tracers of the halo population, globular clusters, RR Lyrae stars, and high-velocity stars, suggest a nonrotating spheroidal component. X-ray observations of galaxies which measure the shape of their potentials also demonstrate the presence of a nonluminous spheroidal component.

For most of this paper, we will assume that the halo distribution function is a truncated exponential

$$f(v_{par}, \mathbf{v}_{perp}) = \exp\{-[(v_{par}-v_t)^2 + \mathbf{v}_{perp}{}^2]/v_c{}^2\}$$

$$\times dv_{par} d\mathbf{v}_{perp}{}^2 \ , \qquad (15)$$

that is cut off at the local escape velocity. v_{par} is the velocity component parallel to Earth's motion and $\mathbf{v}_{perp}$ is the perpendicular component. v_t includes both Earth's motion around the Sun and the Sun's motion through the Galaxy.

We now turn to estimating the escape velocity. Since this will set an upper limit on incident particle velocity, and hence, establish an upper limit on the maximum energy transferred by a particle with a given mass, the escape velocity along with the energy threshold of the detector determines the minimum mass detectable particle.

We will estimate the escape velocity via two routes: (1) we can obtain a lower limit from observation of high-velocity stars; and (2) we can measure the rotation curves of galaxies similar to our own and thus infer their escape velocities.

Observations of high-velocity stars establish only a lower limit on the escape velocity. Limitations of observational searches may make the exponential tail look like the high-velocity cutoff.[7] Recent observational work has attempted to probe the tail of the stellar velocity distribution function. Currently the highest observed stellar velocity is 583 km/sec (Ref. 12). If our halo is composed of weakly interacting particles, we expect that some of the particles will impinge on terrestrial detectors with velocities higher than or on the order of this velocity.

If we assume that the rotation curve of our Galaxy is flat and that our Galaxy extends out to about 100 kpc (as observed in other galaxies), we can estimate the local escape velocity:

$$v_{esc}{}^2 = 2v_c{}^2 \left[\ln \left[\frac{r_{edge}}{r_{local}} \right] + 1 \right] \ , \qquad (16)$$

where r_{edge} is the radius of the Galaxy and r_{local} is the distance between our Sun and the galactic center. This method yields $v_{esc} \approx 625$ km sec^{-1}, consistent with the observational lower limit.

Now we turn to calculating the flux rate of *detectable* particles. Simple kinematics establishes the amount of energy transferred by an incident particle with mass m and velocity v to a detector composed of nuclei of mass M, see Eq. (2). A fraction of the collision of particles with velocities greater than v_{min}, $g(v)$, will result in sufficient energy transferred to produce a detection,

$$g(v) = \frac{\int_{-1}^{\cos\theta_{th}} \sigma(\theta) d\cos(\theta)}{\int_{-1}^{1} \sigma(\theta) d\cos(\theta)} \ , \qquad (17)$$

where θ is the scattering angle, $\sigma(\theta)$ is the scattering cross section, and $\cos(\theta_{th}) = 1 - 2v_{min}{}^2/v^2$. The cases of interest are isotropic, thus,

$$g(v) = 1 - \frac{v_{min}{}^2}{v^2} \ . \qquad (18)$$

We can now integrate over the dark-matter density distribution to determine the predicted count rate per kg per day:

$$R = \frac{6 \times 10^{26}}{A} n_{halo} \int_{v_{min}}^{v_{max}} dv_{perp}{}^2 dv_{par} f(v) \sigma(\mathbf{v})$$

$$\times \left[1 - \frac{v_{min}{}^2}{v^2} \right] |v| \ , \qquad (19)$$

where A is the atomic weight of the material that makes up the superconducting grain. v_{min} contains all of the information about particle mass m, and the capabilities of the detector through E_{th}. The count rate per SQUID per day is found by multiplying R by the mass of the detector inside the SQUID in kg [see Eq. (10)].

IV. THE PARTICLES

Viable candidates for massive, weakly interacting particles which could make up a dark galactic halo are massive neutrinos and the lightest (and therefore stable) supersymmetric particle. In this section we present elastic scattering cross sections for these particles, describe their interactions with the nuclei in the detector, and in each case discuss the viability of detection. We will assume that the candidate particle is present in sufficient abundance to provide the dark halo matter ($\rho_{halo} \approx 0.007 M_\odot/\text{pc}^3$) and is described by a Maxwellian velocity distribution as in Sec. II. We note that particles trapped in our Galaxy move with velocities less than 600 km/sec $= 2 \times 10^{-3} c$ and hence can be treated as nonrelativistic.

In the remainder of this paper we set $h = c = 1$. We will consider momentum transfer in a collision of at most $O(10 \text{ MeV}/c)$. The de Broglie wavelength corresponding to this momentum is $k^{-1} \approx 2 \times 10^{-12}$ cm, larger than the radius of any nucleus, $R \approx 10^{-13}$ cm. Since $kR \ll 1$, the incoming particle interacts with a point nucleus, and one can ignore the finite size of the nucleus and its quark substructure.[13] This assumption begins to break down for particles of mass > 30 GeV; a more detailed analysis would then be required.

A. Massive neutrinos

Neutrinos with large masses occur naturally in a variety of grand unified models[14] and have been invoked in attempts to explain recent anomalous monojet events reported by the UA1 Collaboration.[15] Lee and Weinberg[16] calculated the annihilation cross section for heavy Dirac leptons due to $V - A$ interactions, and derived a lower bound of $4 h_{50}{}^{-1}$ GeV in order that the mass density of neutrinos today does not exceed twice the critical density. h_{50} is the Hubble constant in units of 50 km sec^{-1}Mpc^{-1}. Alternatively, massive neutrinos may be Majorana fermions. In this case there can be significant suppression of s-wave annihilation and the bound on the neutrino mass becomes about 12 GeV (Ref. 17).

Goodman and Witten[2] have calculated the scattering rate in the nonrelativistic limit for any particle that scatters off of nuclei by Z exchange. Their results apply both to massive Dirac neutrinos and to supersymmetric scalar neutrinos. They find a cross section for scattering of a neutrino of mass m off of a nucleus of mass M with z protons and n neutrons:

$$\sigma_{sv_D} = \frac{m_v^2 M^2}{2\pi(m_v + M)^2} G_F^2 Y^2 [z(1 - 4\sin^2\theta_W) - n]^2 , \quad \text{(20a)}$$

where G_F is the Fermi constant and Y is the weak hypercharge ($=1$). Note that in this regime of large de Broglie wavelength, the scattering is coherent, and the cross section is given by the scattering off of one nucleon times a factor

$$\bar{n}^2 = [z(1 - 4\sin^2\theta_W) - n]^2 .$$

For the massive nuclei that we consider in this paper, axial-vector contributions are at most a few percent. We used this cross section in Eq. (19) to find the count rate/kg day and the count rate/SQUID day. In Figs. 3 and 4 we have plotted the count rate/SQUID day as a function of SQUID noise for tin detectors with read-out loops of radius 10 and 20 cm, and for a range of neutrino masses. We see that if the halo is composed of massive Dirac neutrinos, a single SQUID should observe several thousand counts per day if the massive Dirac neutrino mass lies above the detectable mass threshold. Nondegenerate Dirac neutrinos more massive than 9 GeV would produce an observable signal in proton-decay detectors and thus cannot be the dark matter of the halo.[18]

Massive Majorana neutrinos scatter only through spin-dependent interactions. Their cross section for scattering off of nucleons

$$\sigma_{sv_M} = \frac{G_F^2}{8\pi} \frac{m^2 M^2}{(m + M)^2} \lambda^2 J(J + 1) \quad \text{(20b)}$$

is much smaller than that of massive Dirac neutrinos, and similar to photinos, which also have axial-vector couplings. λ is a nucleus dependent factor and J is the magnitude of the nuclear spin (see discussion below).

B. Supersymmetric candidates

Supersymmetric theories predict higher-mass partners for the known particles. The conservation of a new quantum number, R parity, implies that the lowest-mass supersymmetric particle (LSP) should be stable against decay. Depending on various parameters in the theory, the LSP may be the scalar, supersymmetric neutrino ν, the photino $\tilde{\gamma}$, the Higgs fermion S^0, or a mix of $\tilde{\gamma}$ and S^0 combined.[19]

In many theories, the LSP is the photino. If the scale of supersymmetry breaking is related to the weak scale the photino mass is $O(\alpha M_W)$. Cosmological constraints[20,21] establish a lower limit on its mass of 1.8 GeV for $m_{\tilde{q}} \geq 40$ GeV. Photinos couple through axial-vector couplings to leptons via scalar-lepton (supersymmetric lepton) exchange, and to quarks via scalar-quark exchange. The masses of the scalar leptons and scalar quarks that mediate both annihilation and scattering are constrained by experiment to exceed 40 GeV (UA1 Collaboration).

Because of their purely axial-vector coupling to quarks in the simplest models, the scattering of photinos off of individual nuclei adds destructively; hence, the cross section does not have the $\bar{n}^2$ factor due to coherence that was found in the vector coupling case. (We already saw that neutrinos have this factor because of their vector coupling.) Goodman and Witten[2] show that for spin-dependent photino-nucleus scattering cross section can be written as

$$\sigma_{s\tilde{\gamma}} = \frac{m_{\tilde{\gamma}}^2 M^2}{\pi(m_{\tilde{\gamma}} + M)^2} \frac{4q_f^4}{m_f^4} \lambda^2 J(J + 1) , \quad \text{(21)}$$

where f ranges over u and d, J is the magnitude of the nuclear spin, $m_{\tilde{f}}$ is the mass of the scalar quark exchanged in the scattering, q_f is the charge of its quark partner, and λ is a nucleus dependent factor.

In the nuclear shell model,[22]

$$\lambda = 0.55 \left[1 + \frac{s(s+1) - l(l+1)}{j(j+1)} \right] , \quad \text{(22)}$$

where s, l, and j are the spin, orbital, and total angular momentum of the extra proton, neutron, or holes. In Table I we have listed the values of $\lambda^2 j(j + 1)$ for several elements.

FIG. 4. Same as Fig. 3 for scalar or massive neutrinos with a 10-cm loop radius.
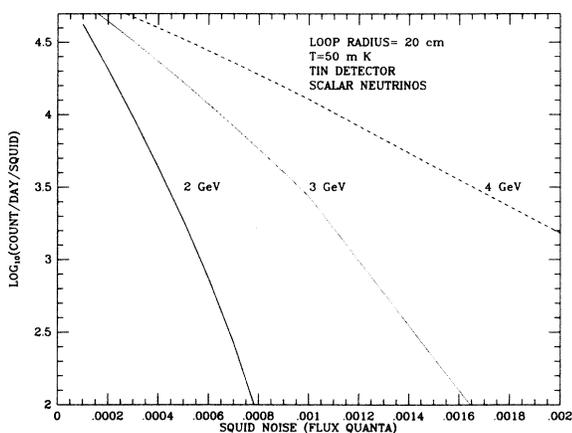

FIG. 3. Expected count rate/day SQUID for scalar or massive neutrinos in a tin detector with 20-cm loop radius at an operating temperature of 50 mK. Count rates for 2, 3, and 4 GeV particles are plotted as a function of read-out system noise in units of flux quantum.
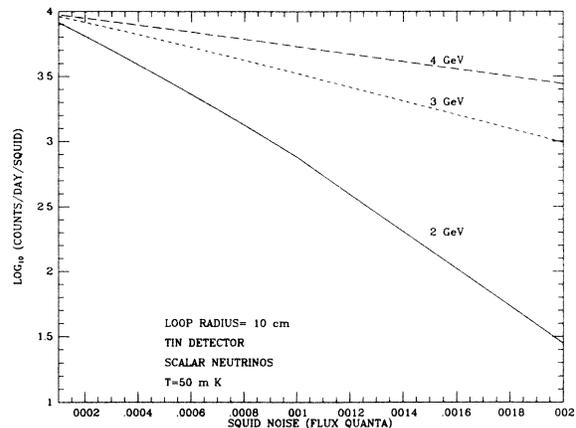
TABLE I. Different elements as photino detector. Following Ref. 2, we tabulate $\lambda^2 J(J+1)$ for various superconducting elements. In parentheses we indicate whether scattering is from up or down quarks and describe the assumed shell-model input. The last column lists the figure of merit as defined in formula (24). We also include data for two semiconductors Si and Ge which could be used as low-temperature bolometers. Unfortunately, the low isotropic abundance of odd nuclei (see second column) makes Si and Ge unattractive for photino detection. Furthermore, we include several light elements that can be used as photino detectors. ^{3}He, ^{7}Li, ^{9}Be, and ^{11}B are commercially available as pure isotopes; enriched abundances are assumed. Abundances for other elements are natural.

Element	(Odd nuclei) (%)	$\lambda^2 J(J+1)$	(u/d)	(Shell model) (shell-model quality)		Figure of merit
^{3}He	100	0.91	d	$s^{1/2}$	neutron hole (good)	0.30
^{7}Li	100	0.50	u	$p^{3/2}$	proton (good)	1.15
^{9}Be	100	0.50	d	$p^{3/2}$	neutron hole (good)	0.06
^{11}B	100	0.50	u	$p^{3/2}$	proton hole (good)	1.53
^{13}C	1.1	0.10	d	$p^{1/2}$	neutron (good)	3.8×10^{-4}
^{15}N	0.36	0.10	u	$p^{1/2}$	proton (good)	0.11
^{17}O	0.04	0.42	d	$d^{5/2}$	neutron (good)	9.9×10^{-6}
^{19}F	100	0.91	u	$s^{1/2}$	proton (good)	0.77
^{27}Al	100	0.42	u	$d^{5/2}$	proton hole (good)	0.25
^{29}Si	4.7	0.91	d	$s^{1/2}$	neutron hole (good)	0.001
^{51}V	99.8	0.40	u	$f^{7/2}$	proton (good)	0.13
^{67}Zn	4.11	0.22	d	$f^{5/2}$	neutron hole (good)	0.001
^{69,71}Ga	100	0.50	u	$p^{3/2}$	proton (fair)	0.11
^{73}Ge	7.76	0.37	d	$g^{9/2}$	neutron (good)	0.0004
^{93}Nb	100	0.37	u	$g^{9/2}$	proton (good)	0.06
^{103}Rh	100	0.10	u	$p^{1/2}$	proton (fair)	0.02
^{111,113}Cd	25	0.36	d	$h^{11/2}$	neutron	0.0008
		0.91	d	$s^{1/2}$	neutron (both models poor)	0.002
^{113,115}In	100	0.37	u	$g^{9/2}$	proton hole (fair)	0.05
^{115,117}Sn	16.5	0.36	d	$h^{11/2}$	neutron	0.0005
		0.91	d	$s^{1/2}$	neutron (both models poor)	0.001
^{203,205}Tl	100	0.18	u	$s^{1/2}$	proton	0.01
		0.91	u	$d^{3/2}$	proton (both models poor)	0.07
^{207}Pb	22.6	0.10	d	$p^{1/2}$	neutron hole (good)	0.0001

There may be mixing between left- and right-handed scalar quarks.[2] This is not favored in most models. If such mixing did exist, photinos would couple coherently to quarks with cross sections proportional to $(2n+z)^2$ for a d scalar quark and $(2z+n)^2$ for a u scalar quark. This coupling depends upon the mixing angle β, which is limit-

ed to be quite small; therefore, coherent scattering is not significant.

Photinos are Majorana particles, and like Majorana neutrinos, their s-wave annihilations are suppressed. The photino annihilation rate has been calculated in the nonrelativistic limit[20,21] to be

$$(\sigma_a \mid v \mid)_{\tilde{\gamma}} = \frac{1}{2\pi} \sum_f q_f^4 \left[1 - \frac{m_f^2}{m_{\tilde{\gamma}}^2} \right]^{1/2}$$

$$\times \left[\frac{1}{3} \frac{m_{\tilde{\gamma}}^2 - m_f^2}{m_{\tilde{f}}^4} \mid v \mid^2 + \frac{m_f^2}{m_{\tilde{f}}^4} \right] .$$

(23)

The sum f ranges over the quarks $(u, d, s, c,$ etc.) with $\tilde{f}$ the corresponding scalar quarks, and over the leptons (and corresponding scalar leptons). In the range we are interested in $(M_{\tilde{\gamma}} \approx 50$ GeV$)$, the scalar-quark masses must generally be degenerate.[23] Otherwise their contribution to the K^0-$\overline{K}^0$ mixing is not canceled by the Glashow-Iliopoulos-Maiani (GIM) mechanism, leading to a large K_L-K_S mass splitting, in conflict with observation.

Since today the density of photinos $\rho_{\tilde{\gamma}} \propto 1/(\sigma v)_{min}$, for different values of photino mass one can calculate the scalar-quark mass required to achieve $\Omega_{\tilde{\gamma}} = 1$ (see Fig. 6). Again applying Eq. (19), one can obtain the count rate kg day and rate/SQUID day, which are plotted in Figs. 5 and 6 as a function of SQUID noise for various values of photino mass in an aluminum detector with read-out loops of radius 10 and 20 cm.

The scalar neutrino, the supersymmetric partner of the neutrino, can also be the LSP (Ref. 20). Since it has vector couplings to Z bosons and scatters from nuclei by Z exchange, its cross sections are identical to the massive neutrino. Hence, the neutrino scattering cross sections of Goodman and Witten can be used with m_ν replaced by $m_{\tilde{\nu}}$. The same count rate in the detector is obtained as for massive neutrinos (see Fig. 4).

The scalar neutrino's cosmological annihilation, however, is very different from that of the massive neutrino. For most parameter choices, annihilation via exchange of neutral gauge/Higgs fermions[24] dominates over other annihilation channels. This annihilation rate, because of its fermionic propagator, is very rapid: for most parameter
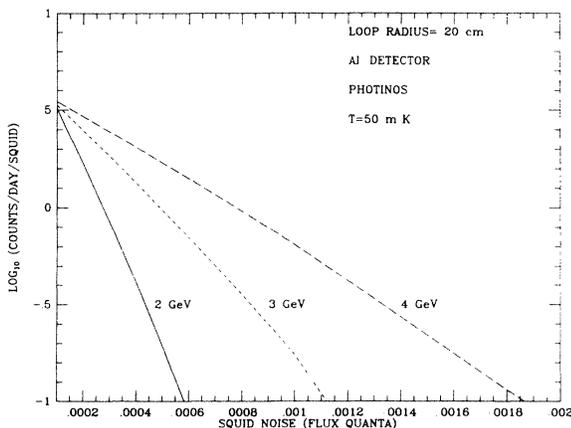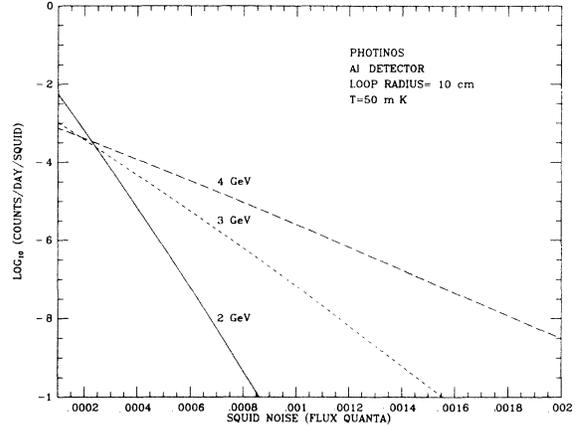

FIG. 6. Same as Fig. 3 for photino count rate in Al detector with 10-cm loop radius.

choices, the scalar-neutrino cosmological density will be much less than its closure density. With fine-tuning,[25] this annihilation mechanism can be suppressed and scalar neutrinos can close the Universe. Limits from the decay of scalar neutrinos captured by Earth establish that scalar neutrinos more massive than 12 GeV cannot provide the dark matter of the halo.[18]

V. THE BACKGROUND

In the previous section, we saw that a 1-kg detector sensitive to 50-eV recoils should record 10^4 counts per day if the galactic halo is composed of scalar or massive neutrinos of mass greater than 4 GeV and a few counts per day if photinos are the dominant component of the missing mass. In this section, we will discuss the various sources of background: cosmic rays, natural radioactivity, and solar neutrinos.

The μm granularity, reasonable energy resolution, and μsec time resolution of the detector permit excellent background rejection. The signature of a neutral scattering event is the flipping of one and only one grain. In a solar neutrino detector,[1] natural radioactivity is the dominant background source $(\approx 5 \times 10^{-3}$ counts/kg day$)$. For our dark-matter detector, the solar neutrinos are a background component.

The cosmic-ray background flux has been discussed in previous studies of SSCD's (Ref. 1). At the Earth's surface, hundreds of muons will cross the grains every day. A simple external veto detector, however, can suppress this background by a factor of a thousand. Most of the muons will flip multiple grains, and thus will be rejected as background; only very few muons will flip only one grain. At a depth of 1500 m.w.e. (metric water equivalent), muons are expected to contribute 6.6×10^{-3} counts/kg day and at a depth of 4000 m.w.e., only 6.0×10^{-5} counts/kg day.

Radioactive contamination by natural elements (^{40}K, U, and Th) can be reduced below one part per billion with chemical purification techniques. U and Th contamination are the easiest to control; ^{40}K will be the major con-

FIG. 5. Same as Fig. 3 for photino count rate in Al detector with 20-cm loop radius.

taminant. In 1 kg of tin contaminated by one potassium atom per 10^8, there are 1.5×10^{17} K atoms and 1.8×10^{14} atoms of radioactive ^{40}K atoms. ^{40}K is a β^- emitter with a lifetime of 4.73×10^{11} day. Thus we expect 260 decays/day. Since E_{max} (^{40}K) ≈ 1.4 MeV, most of the emitted electrons will flip hundreds of grains. The energy range corresponding to that of electrons that flip only one grain is $E_{\beta^-} < 10$ keV. Only 10^{-5} of all ^{40}K decays will produce a change of state in just one grain, thus the expected radioactive background for material of purity one part in 10^8 is 2.6×10^{-3} counts/kg day. Active experimental programs at the University of South Carolina, Columbia, and Max-Planck Institut, Munich are pursuing the reduction of radioactive background.

State-of-the-art purification techniques can further reduce the level of impurities in metals with low melting points such as tin. Zonal refining techniques, similar to those used for Si and Ge, may reduce the contamination by several orders of magnitude below our assumed value to purity levels comparable to commercially available Si ingots ($\approx 10^{-12}$). Chemical purity, however, is not synonymous with radio purity. Careful analysis of the detector materials for the existence of long-lived radioisotopes is essential for background reduction. Long-lived isotopes, such as ^{32}Si and ^{26}Al, are a major source of background for silicon-based or sapphire-based bolometric detectors.[26] The experimental studies show that commercially available Si crystals have 3—4 orders of magnitude higher radioactive background than very pure Sn or Pb. The present available material is Ge.

The SSCD will also detect solar neutrinos. Solar neutrinos will scatter both coherently off of nuclei and off of electrons in the grain. For coherent scattering off of nuclei, the neutrino count rate depends strongly on the energy threshold. When searching for particles with masses > 10 GeV, an energy threshold of 200 eV permits detection and allows only ^{8}B neutrinos to contribute to the background ($< 5 \times 10^{-4}$/kg day). However, detection of particles of lower mass requires a lower energy threshold. A 50-eV threshold, low enough to detect 2-GeV particles, will allow both ^{7}Be and ^{8}Be to contribute to the background ($\approx 5 \times 10^{-3}$ counts/kg day).

Neutrino scattering off of electrons in the grain will also contribute to the background. The abundant p-p neutrinos will be the dominant source. The total contribution of neutrons-electron scattering[1] to the background is less than 2×10^{-3} counts/kg day).

If the galactic halo is composed of either scalar neutrinos or photinos of masses greater than 2 GeV, the dark-matter count rate should dominate over the background by several orders of magnitude. A conservative estimate of background is $(1-5) \times 10^{-3}$ counts/kg day. For low-energy thresholds, the solar neutrinos are the dominant component of the background. For higher-energy thresholds, radioactive impurities are expected to be the major background source.

Since the typical background particle deposits far more energy than one of the dark-matter candidates, the background count rate should be insensitive to the energy threshold. Cosmic-ray muons and electrons emitted from the β^- decay of ^{40}K deposit 1.5 keV/μm of tin. Thus,

they would deposit ≈ 5 keV in a 2-μm grain. The coherent scattering of a solar neutrino off of the electrons in the grain will deposit about 10 keV. On the other hand, the typical dark-matter candidate with $m < 20$ GeV will deposit less than 1 keV in a collision. Thus, a simple way to reject background is to run the SSCD detector with two different energy thresholds, say 0.5 and 2 keV. This change of threshold will not significantly change the background contribution to the count rate but should practically eliminate all events due to dark-matter candidates.

The motion of Earth around the Sun produces a modulation in the dark-matter count rate (see Fig. 7). This modulation will enhance our ability to subtract off background, and help confirm a detection. The modulation effect is greatest when the energy threshold lies just below the maximum possible energy transferred in a collision. In this regime, the effects of adding (or subtracting) Earth's motion around the Sun is significant. When Earth's velocity relative to the halo is highest, there are more particles above the energy threshold. (Note that the ecliptic is inclined by 62.5 deg from the galactic plane, thus only a fraction of Earth's velocity is added to the heliocentric velocity.)

This predicted modulation is not the result of our assumed velocity distribution nor is it very sensitive to instrument imperfections. We expect this effect for any velocity distribution that has a cutoff at high velocity. Since particles with velocities greater than the Galaxy's escape velocity would have escaped long ago, a cutoff is inevitable. Instrument imperfections will only slightly reduce the amplitude of this modulation. For example, variations in grain sizes or diamagnetic effects between grains may produce a spread in the energy threshold of $\Delta E_{th}/E_{th} \leq 0.1-0.5$. The Appendix discusses the dependence of the modulation effect on the shape of the distribution function and the width of the energy threshold.

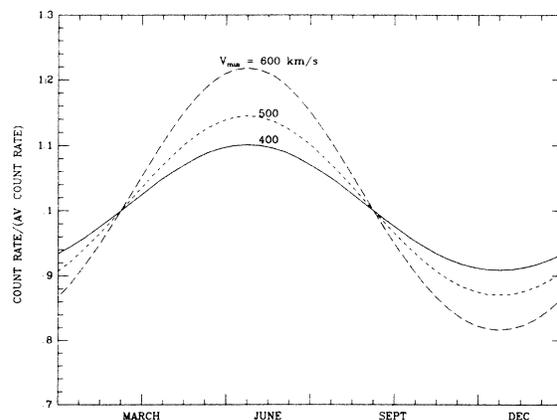We also expect a modulation in the solar-neutrino con-

FIG. 7. Modulation of dark-matter signal in the detector due to the motion of the Earth around the Sun. Expected count rate/(averaged count rate) is plotted for different months of the year. This modulation effect can be used to enhance background subtraction.

tribution to the background. As the Earth-Sun distance undergoes its annual variation, the solar-neutrino count rate varies as $1/R(t)^2$. When Earth is closest to the Sun in January, the solar-neutrino contribution to the background will be at its maximum. The halo dark-matter count rate should be at a maximum in May when the Earth's velocity around the Sun is parallel to the Sun's motion around the galactic center.

VI. PARTICLE DETECTION AND IDENTIFICATION

What we can detect will depend upon the energy threshold of the detector and the noise level in the SQUID. In Fig. 8 we have plotted the minimum detectable mass for various particles as a function of operating temperature (here loop radius is assumed to be 20 cm and SQUID noise $5\times10^{-4}\phi_0$). At an operating temperature of 50 mK, neutrinos or scalar neutrinos with masses above 2 GeV should be seen in a tin detector with a large count rate of 50 counts/day. 7-GeV scalar neutrinos would produce 10^5 counts/day. If massive or scalar neutrinos compose the "missing mass" of the halo, we anticipate signal-to-background ratios in excess of 10^4. Photinos more massive than 2 GeV could be seen with a lower count rate of 0.5 counts/day, still 10^2 higher than the anticipated background count rate. The annual modulation in the signal due to the Earth's motion and the energy dependence of the signal will capacitate significant enhancement of the signal-to-background ratio.

The next question we wish to address is that of particle identification. Once the detector responds to some type of massive particle, how can we identify the particle? We will show that one can determine the mass and the type of coupling of the incoming particle by varying the energy threshold and the material of the detector.

Changing the applied magnetic field or the operating temperature varies the energy threshold. As the threshold rises, fewer particles carry enough energy to change the state of the detector grains, and hence the count rate decreases. Just before the threshold energy is so high that the signal disappears altogether, only the very fastest particles can still flip the grain ($v_{min}=v_{esc}\simeq600$ km/sec), and from Eq. (16) one can obtain an estimate of the mass of the particle.

Recall that many different elements can be used for grains in the detector (see Table I). By using detectors composed of several different materials, we can determine the mass and coupling of the particle. Photinos, because they couple only through an axial-vector coupling, will not scatter off of even-even nuclei. Since the photino-nucleon scattering cross section scales as the fourth power of quark charge, the predicted count rates are much higher for elements which couple through an up scalar quark ($q_f=\frac{2}{3}$) than for those which couple through a down scalar quark ($q_f=\frac{1}{3}$). Table I lists a figure of merit for several superconductors and for silicon and germanium semiconductors that have also been proposed for use in particle detectors.[27] In the limit $m_{\tilde{\gamma}}\ll M$, the predicted photino count rate scales as the figure of merit F_M:
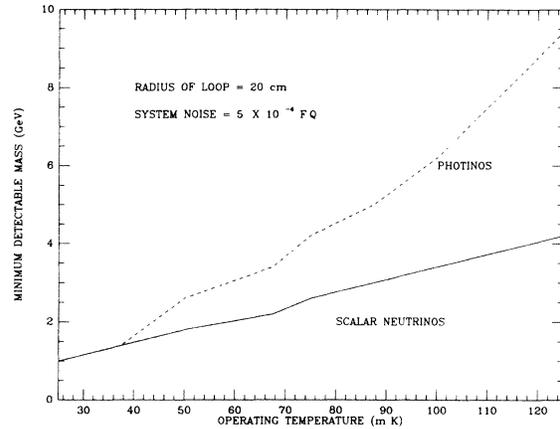

FIG. 8. Minimum detectable mass for both photinos and scalar (or massive) neutrinos as a function of system temperature. In this plot we assume a system noise of $5\times10^{-4}\phi_0$ and a 20-cm detector loop. For masses greater than the minimum detectable mass, we expect at least 0.5 counts/day SQUID if photinos compose the halo and 100 counts/day SQUID if scalar (or massive) neutrinos compose the halo.

$$F_M = f_{odd}q_f{}^4\frac{\lambda^2 J(J+1)}{M} ,\qquad(24)$$

where f_{odd} is the natural fractional abundance of nuclei with odd atomic weights for a given element. Note that Si and Ge do not couple efficiently to photinos. By using pairs of elements with similar superconducting properties, but drastically different isotopic composition, we can determine if the particle couples through an axial-vector (photino) or a vector (massive or scalar-neutrino) coupling. There are several such promising elemental pairs: Zn and Ga, In and Sn, as well as Tl and Pb. For example, the count rate for a particle that couples with axial-vector couplings in a gallium detector is 100 times higher than its count rate in a similar zinc detector. While, on the other hand, the count rate will be similar in both detectors for particles with vector couplings.

The mass dependence of the cross section allows the determination of particle mass through the use of several different detectors. Recall that for vector coupling,

$$\sigma\propto\frac{mM}{(m+M)^2}\bar{n}^2 ,\qquad(25)$$

while for axial-vector coupling,

$$\sigma\propto\frac{mM}{(m+M)^2} .\qquad(26)$$

Once the type of coupling has been identified, several detectors with masses in the range $M\sim m$ can then be used to extract the particle mass.

VII. CONCLUSIONS

We have examined the viability of the use of superheated superconducting colloids as detectors of weakly interacting massive particles. Our analysis can easily be extended to other candidate detectors (see Ref. 27) and to other particles of comparable cross section. If the missing

mass of the Galaxy is composed of massive (several GeV) particles that interact with nuclei through the exchange of Z^0's, scalar quarks, or other intermediate particles of like masses and couplings, SSCD's can be used to detect these particles. Let us review the candidate particles.

Scalar and massive neutrinos. Because of their dominantly vector coupling with quarks, these particles scatter coherently off of nucleons. If these particles compose the halo, a 1-kg tin detector should be able to record thousands of events per day.

Photinos. These particles couple with quarks through axial-vector couplings; therefore, little is gained by building a detector out of grains of one of the more massive type-I superconducting elements. We find that if these particles compose the halo and their mass is above the minimum threshold, we can anticipate a 1-kg Al detector recording approximately one count per day. Figure 9 shows the experimental and cosmological limits on photino and scalar-quark masses. The UA1 Collaboration has established a lower limit on scalar-quark mass of 40 GeV. Cosmology sets a lower limit on photino mass as a function of scalar-quark mass. If photinos are captured during galaxy formation (it is difficult to avoid their accretion into collapsing proto-galaxy), they should be detectable by an Al SSCD if system noise is reduced below 5×10^{-4} flux quanta and the system is maintained at 50 mK (see however discussion of ^{26}Al below).

Alternatively, low-temperature bolometers can be used to detect photinos.[27] The need for materials with very low specific heat suggests crystals with very high Debye temperature θ_D. Cubic lattices have the best thermal properties. Familiar crystals with cubic lattices are diamond, $\theta_D = 2200$ K, sapphire, $\theta_D = 900$ K, silicon, $\theta_D = 645$ K, and germanium, $\theta_D = 373$ K. On the other hand, as long as $m < M$, photino cross sections are higher for light materials than for heavier nuclei (see Table I).
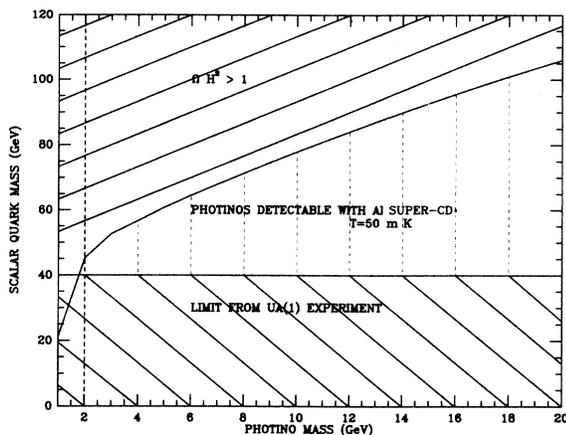

FIG. 9. Detector capabilities. Scalar-quark mass (in GeV) is plotted as a function of photino mass (in GeV). Cross-hatched regions are excluded by present limits: the scalar-quark mass is constrained by the UA1 Collaboration to exceed 40 GeV, and the requirement that $\Omega H_0{}^2 < 1$ demands a photino mass greater than 1.8 GeV. The SSCD can then detect photinos or rule the region in dashed lines.

Radioactive background is a major consideration in designing semiconductor dark-matter detectors. Silicon, unfortunately, has an isotope (^{32}Si) that is a β^- emitter with a 100 yr half-life and $E_{max} \approx 210$ keV. Its daughter ^{32}P is also a β^- emitter with $t_{1/2} = 14.3$ d and $E_{max} = 1.71$ MeV. For example, in very pure silicon extracted from seawater, the radioactive background due to ^{32}Si was observed to be ~ 30000 counts/kg day (Ref. 28). Sapphire contains ^{26}Al, a β^+ emitter with $t_{1/2} = 6.4 \times 10^5$ yr and $E_{max} = 1.16$ MeV. Fortunately, the positron annihilation that follows the β^+ decay produces a very specific signal that can be used to reject most of the ^{26}Al contribution to background.

Boron ($\theta_D = 1480$ K) and boron compounds (e.g., boron nitride, $\theta_D = 780$ K and boron phosphide, $\theta_D = 780$ K) are attractive materials for bolometric photino detectors as is LiF ($\theta_D = 750$ K). Thermal neutrons may, unfortunately, produce a significant background. We will discuss the boron-, lithium-, and fluor-based detectors in a subsequent paper.[29]

"Technibaryons." Nussinov[30] has suggested that the missing matter is in the form of technibaryons and that these particles have scattering via Z exchange and have masses in the TeV range. Since the technibaryon-nucleon cross section is the same as the scalar-neutrino—nucleon cross section, these particles can also be easily detected if they compose the halo.

"Cosmions." Press and Spergel[31] showed that if the halo was composed of weakly interacting particles, the Sun would capture these particles. In the Sun, these particles could transport energy and resolve the "solar-neutrino problem."[32] These particles must have masses greater than 4 GeV if they are to remain trapped in the Sun. They must either have annihilation cross sections at low energies suppressed by a factor of 10^{-5} relative to their scattering cross section off of nucleons or have a net asymmetry either between cosmion and anticosmion number or between cosmion-baryon and anticosmion-baryon scattering.[33] If these particles couple coherently to matter, their scattering cross section with helium must be $\sim 4 \times 10^{-36}$ cm^2 if they are to solve the solar-neutrino problem. If the cosmions have axial-vector coupling to matter, the ideal scattering cross section with hydrogen is $\sim 2 \times 10^{-36}$ cm^2. For comparison, consider that the scattering cross section of a 5-GeV scalar neutrino off of helium is 1.2×10^{-37} cm^2 and the scattering cross section of a 5-GeV photino off of hydrogen is $\sim 6 \times 10^{-37}$ cm^2. Thus if the cosmion couples through vector interactions, its scattering cross section must be greater than or on order of that of scalar neutrinos and if the particle couples through spin interactions, its scattering cross section must be greater than that predicted for a photino if the scalar quark has mass of at least 30 GeV. In either case, we expect the detector to be capable of observing the particles. *If the halo is composed of weakly interacting particles that alter the thermal structure of the Sun, their scattering cross sections must be sufficiently large so as to be detectable by low-temperature detectors.*

"Shadow Matter." Recently it was pointed out[34,35] that the dark matter in our Galaxy may be made of a variety of shadow matter which interacts with ordinary matter.

The simplest "shadow world" has a single stable particle carrying shadow charge, together with massless shadow photons. The "shadow particles" can interact with normal matter and cross sections can be as large as 10^{-28} cm^2. These particles would be detectable with SSCD's as small as a few grams. However, it seems possible that also very-low-background semiconducting detectors can place limits on these particles.[36]

"*Axions, Familons Majorons:*" There are arguments in theoretical elementary particle physics for the proliferation of types of neutral weakly interacting particles with very small mass, e.g., axions,[37] Majorons,[38] and familons.[39] They would be good candidates for "hot dark matter." Furthermore, they would be produced in the Sun. Because these new particles tend to interact so weakly, some enhancement mechanism must be relied on to detect them. Axions, Majorons, and familons interact with electrons; it was shown[40] that the atomic bound-state effects lead to great enhancements (10^5-10^6) in the detection rate. The required detectors should be able to measure energy depositions as small as atomic energies and should have very low background. Obviously, SSCD could detect solar axions, familons, or Majorons but there is no advantage in using low-temperature detectors. The semiconducting detectors would work as well as SSCD providing the same energy sensitivity and radioactive background.[41,42]

The level of system noise and the system temperature sets a minimum energy threshold. For a scattering event to be recorded, the recoil energy of the nucleus must exceed this minimum energy threshold. Since there is a cutoff in the velocity of particles that compose the halo, the energy threshold implies a minimum detectable particle mass. If the system is maintained at 50 mK and the system noise is reduced below 5×10^{-4} flux quanta, the detector is capable of recording collisions of any halo candidate particle whose mass exceeds 2 GeV. Note that the scalar-quark mass is known to exceed 40 GeV, the minimum photino mass is 1.8 GeV.

Natural radioactivity is expected to be the major source of background. Because the detector is sensitive to the number of grains flipped, excellent background subtraction is possible. A weakly interacting halo particle will flip only one grain; most background sources will flip multiple grains. The background count rate is expected to be less than 5×10^{-3} events/day, several orders of magnitude less than the predicted count rate for the candidate particles.

The Earth's motion around the Sun will produce a distinctive modulation in the signal detected from halo particle candidates. This modulation effect will be important in any dark-matter detector with reasonable energy resolution. Adjusting the minimum threshold will increase the amplitude of this annual oscillation. Background rates due to natural radioactivity should be time independent. This modulation in the signal is out of phase with the modulation in the solar-neutrino contribution to the background due to the variation in the distance between the Sun and the Earth and any modulation in the background due to the changes in the tilt of the Earth's axis relative to the ecliptic. This signal modulation will allow additional confirmation of detection.

We see that superheated superconducting colloids are capable of detecting several dark-matter candidate particles. SSCD's have the possibility of making visible the "invisible" dark matter that may compose 90% of the Universe.

Finally, we should like to point out that some limits on cold dark-matter candidates have been already obtained using very-low-background germanium spectrometer.[42]

ACKNOWLEDGMENTS

APPENDIX

Since the modulation effect is very useful in eliminating background and confirming a detection, it is useful to show its universality for a distribution function that reproduces the observed r^{-2} halo and its insensitivity to the details of the detector response near its energy threshold.

The count rate per kilogram per day R depends upon the cosmion distribution function $f(\mathbf{v})$ and $h(E)$, the detection efficiency at energy E.

$$R(t) = \frac{6 \times 10^{26}}{A} n_{\text{halo}}$$

$$\times \int d^3v \int_{-\pi}^{\pi} f(\mathbf{v},t) h(E(v,\xi)) \sigma(E) d\xi . \quad \text{(A1)}$$

A is the atomic number of the nuclei that compose the detector and ξ is the scattering angle. $h(E)$ equals 1 when all scatters of energy E produce detectable signals in the electronics. Equation (A1) reduces to Eq. (19) when $h(E-E_{\text{th}})$ is a Heaviside function.

We will model the detector as having an energy threshold E_{th} of width ΔE_{th}. All scatters that deposit more than $E_{\text{th}} + \Delta E$ produce a signal and all scatters that deposit less than $E_{\text{th}} - \Delta E$ go undetected. Near the threshold, the response is assumed to be linear:

$$h(E) = \begin{cases} 1, & E \geq E_{\text{th}} + \Delta E , \\ (E - E_{\text{th}} + \Delta E)/2\Delta E, & E_{\text{th}} - \Delta E \leq E \leq E_{\text{th}} + \Delta E , \\ 0, & E \leq E_{\text{th}} - \Delta E . \end{cases}$$

$$\text{(A2)}$$

We can use Eq. (2) to integrate $h(E)$ over scattering angles.

The halo model used in the text can be extended to a generalization of a Michie model. The Michie model is a function of both the particle's energy E and its angular momentum J; thus it allows the velocity distribution function to range from radial through isotropic to circular. Note that in these models the velocity dispersion perpendicular to the disk equals the velocity dispersion parallel to the disk's sense of rotation. The halo's distribution function, locally, in the halo frame f_{halo} is cut off at the escape velocity v_{esc} and has two other independent parameter λ and σ:

$$f_{\text{halo}}(\mathbf{v}) = N \left[\exp\left(-\frac{v_r^2 + v_\phi^2 + v_z^2}{\sigma^2} \right) - \exp\left(-\frac{v_{\text{esc}}^2}{\sigma^2} \right) \right]$$
$$\times \exp\left(-\lambda \frac{v_\phi^2 + v_z^2}{\sigma^2} \right). \tag{A3}$$

v_ϕ is the particle's motion parallel to the disk's rotation, v_z is the particle's motion perpendicular to the disk, and v_r is the particle's radial velocity. N normalizes the distribution function.

To transform from the halo frame to the frame of Earth, we must include the Earth's motion relative to the halo $v_e(t)$. This motion has two components, the Sun's circular motion around the galactic center and the Earth's velocity relative the Sun. It is the latter, the Earth's annual revolution, that is the source of the modulation in count rate. The distribution function in the Earth's frame can be cast in terms of the familiar u, v, and w local standard of rest variables:[43]

$$f(u,v,w) = N \left[\exp\left(\frac{u^2 + [v - v_e(t)]^2 + w^2}{\sigma^2} \right) - \exp\left(\frac{v_{\text{esc}}^2}{\sigma^2} \right) \right]$$
$$\times \exp\left[\lambda \frac{[v - v_e(t)]^2 + w^2}{\sigma^2} \right]. \tag{A4}$$

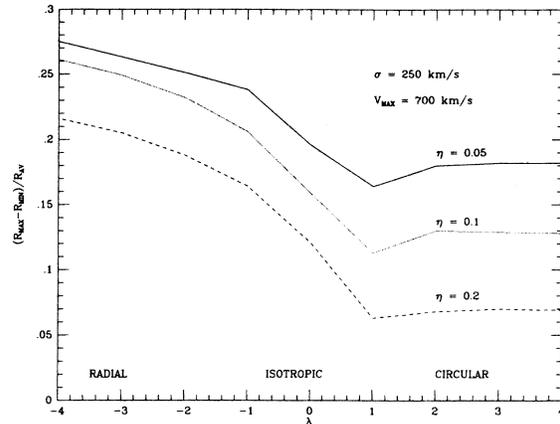Equations (A1), (A2), and (A4) yield the time-dependent count rate.

FIG. 10. Dependence of the dark-matter modulation on the velocity distribution function. The difference between the maximum and minimum count rate normalized to the average count rate is plotted for a range of velocity distribution with the fraction of incident detected η held constant. A reasonable model for the halo might have $-1 < \lambda < 0$.

The amplitude of the signal modulation depends upon the location of the energy threshold. We can adjust the detector energy threshold by changing the magnetic field. A higher-energy threshold reduces the count rate but increases the amplitude of the modulation. Figure 10 demonstrates the dependence of the modulation on the shape of the distribution function with the fraction of the incident flux detected η held constant. Since it was generated by galaxy collapse, the halo velocity distribution function is most likely isotropic to radial. A sharper energy threshold would produce a slightly stronger modulation. The uncertainties in the halo's velocity dispersion and escape velocity do not significantly alter the amplitude of the modulation. This effect is also not strongly sensitive to the width of the energy threshold.

[1]A. K. Drukier and L. Stodolsky, Phys. Rev. D **30**, 2295 (1984); A. K. Drukier, Acta Phys. Pol. (to be published).

[2]M. W. Goodman and E. Witten, Phys. Rev. D **31**, 3059 (1985), see, also, I. Wasserman, *ibid.* **33**, 2071 (1986).

[3]D. J. Hegyi and K. A. Olive, Fermilab Report No. Pub-85/26-A, 1985 (unpublished).

[4]A. Bosma, thesis, University of Groningen, Netherlands, 1978; V. C. Rubin W. K. Ford, and N. Thonnard, Astrophys. J. Lett. **225**, L107 (1978).

[5]J. N. Bahcall and S. Casertano, Astrophys. J. **293**, L7 (1985).

[6]J. H. Oort, Bull. Astron. Inst. Neth. **3**, 275 (1927); J. N. Bahcall, Astrophys. **276**, 169 (1984).

[7]J. Caldwell and J. P. Ostriker, Astrophys. J. **251**, 61 (1981).

[8]J. N. Bahcall and R. M. Soniera, Astrophys. J. Suppl. **55**, 67 (1984).

[9]G. R. Knapp, S. D. Tremaine, J. E. Gunn, Astron. J. **83**, 1585 (1978).

[10]D. Lynden-Bell, Mon. Not. R. Astron. Soc. **136**, 101 (1967).

[11]S. Tremaine, MIT report, 1985 (unpublished).

[12]D. Latham (private communication).

[13]D. V. Freedman, D. N. Schramm, and D. L. Tubbs, Annu. Rev. Nucl. Sci. **27**, 167 (1977).

[14]J. Bagger, S. Dimopoulos, E. Masso, and H. Reno, Phys. Rev. Lett. **54**, 2199 (1985).

[15]UA1 Collaboration, M. Gronau and J. L. Rosner, Phys. Lett. **147B**, 217 (1984); L. M. Krauss, Nucl. Phys. **B227**, 556 (1984).

[16]B. W. Lee and S. Weinberg, Phys. Rev. Lett. **39**, 165 (1977).

[17]L. M. Krauss, Phys. Lett. **128B**, 37 (1983).

[18]For a discussion on limits placed on scalar-neutrino masses,

see K. Freese, Phys. Lett. **167B**, 295 (1986); L. Krauss, M. Srednicki, and F. Wilczek, Phys. Rev. D **33**, 2079 (1986).

[19]J. Polchinski, in *Inner Space/Outer Space*, edited by F. W. Kolb, M. S. Turner, K. Olive, D. Seckel, and D. Lindley (University of Chicago Press, Chicago, in press).

[20]J. Ellis, J. S. Hagelin, D. V. Nanopoulos, K. Olive, and M. Srednicki, Nucl. Phys. **B238**, 453 (1984).

[21]H. Goldberg, Phys. Rev. Lett. **50**, 1419 (1984).

[22]M. W. Goodman, and E. Witten (private communication).

[23]G. L. Kane and H. E. Haber, Phys. Rep. **117**, 77 (1985); M. Dugan, B. Grinstein, and L. Hall, Nucl. Phys. B (to be published).

[24]J. S. Hagelin, G. L. Kane, and S. Raby, Nucl. Phys. **B241**, 638 (1984).

[25]J. S. Hagelin and G. L. Kane report (unpublished).

[26]F. Avignone, R. Brodzinski, and E. Fireman (private communication).

[27]H. H. Anderson, C. C. Manke, and H. Sorenson, Rev. Sci. Instrum. **38**, 511 (1967); T. O. Niinikoski and F. Udo, CERN Report No. 74-6, 1974 (unpublished); A. K. Drukier and L. Stodolsky, report, 1982 (unpublished); E. Fiorini and T. O. Niinikoski, Nucl. Instrum. Methods **224**, 83 (1984); S. H. Moseley, J. C. Mather, and D. McCammon J. Appl. Phys. **56**, 1257 (1984), D. McCammon, S. H. Moseley, J. C. Mather, and R. F. Mushotzky, *ibid.* **56**, 263 (1984); B. Cabrerra, L. M. Krauss, and F. Wilczek, Phys. Rev. Lett. **55**, 25 (1985); B. Sadoulet and E. Cummins (private communication); H. H. Anderson, Nucl. Instrum. Methods B **12**, 437 (1985).

[28]D. Lal, E. D. Goldberg, and M. Koide, Science **131**, 332 (1960).

[29]A. K. Drukier, K. Freese, and D. N. Spergel (unpublished).

[30]S. Nussinov, Phys. Lett. **165B**, 55 (1985).

[31]W. H. Press and D. N. Spergel, Astrophys. J. **296**, 679 (1985).

[32]G. Steigman, C. L. Sarazin, H. Quintana, and J. Faulkner, Astron. J. **83**, 1050 (1978); D. N. Spergel and W. H. Press, Astrophys. J. **294**, 663 (1985); J. Faulkner and R. Gilliland, *ibid.* (to be published); R. Gilliland J. Faulkner, W. H. Press,

and D. N. Spergel (unpublished).

[33]L. M. Krauss, K. Freese, D. N. Spergel, and W. H. Press, Astrophys. J. (to be published); L. Hall and G. Gelmini (private communication).

[34]L. J. Hall, in *Supersymmetry and Supergravity/Nonperturbative Q.D.D.*, proceedings of the Winter School at Mahabaleshwar, India, 1984, edited by P. Roy and V. Singh (Lecture Notes in Physics, Vol. 208) (Springer, Berlin, 1984).

[35]H. Goldberg and L. J. Hall, Harvard Report No. HUTP-86/A029, 1986 (unpublished).

[36]A. K. Drukier and D. N. Spergel (unpublished).

[37]R. D. Peccei and H. R. Quinn, Phys. Rev. B **3**, 1440 (1977); Phys. Rev. D **16**, 1791 (1971); S. Weinberg, Phys. Rev. Lett. **40**, 223 (1978); F. Wilczek, *ibid.* **40**, 279 (1978); J. E. Kim, *ibid.* **43**, 103 (1979); M. A. Shifman, A. I. Vainshtein, and V. I. Zaharov, Nucl. Phys. **B166**, 493 (1980); M. Dine, W. Fischler, and M. Srednicki, Phys. Lett. **104B**, 199 (1981); J. E. Moody and F. Wilczek, Phys. Rev. D **30**, 130 (1984).

[38]D. B. Reiss, Phys. Lett. **115B**, 217 (1982); F. Wilczek, Phys. Lett. **49**, 1549 (1982); G. Gelmini, S. Nussinov, T. Yanagida, Nucl. Phys. **B219**, 31 (1983).

[39]Y. Chicashige, R. N. Mohaparata, and R. D. Peccei, Phys. Lett. **98B**, 265 (1981); Phys. Rev. Lett. **45**, 1926 (1980); G. B. Gelmini and M. Roncadelli, Phys. Lett. **99B**, 411 (1981); H. Georgi, S. L. Glashow, and S. Nussinov, Nucl. Phys. **B193**, 297 (1981).

[40]S. Dimopoulos, B. W. Lynn, and G. D. Starkman, SLAC preprint 3850, 1985 (unpublished).

[41]F. T. Avignone III, R. L. Brodzinski, S. Dimopoulos, A. K. Drukier, G. B. Gelmini, B. W. Lynn, D. N. Spergel, and G. D. Starkman, SLAC Report No. 3872, 1986 (unpublished).

[42]S. P. Ahlen, F. T. Avignone III, R. L. Brodzinski, A. K. Drukier, G. Gelmini, and D. N. Spergel, Harvard-Smithsonian Center for Astrophysics Report No. 2292, 1986 (unpublished).

[43]D. Mihalis and J. J. Binney, *Galactic Astronomy* (Freeman, San Francisco, 1981).